PCCP

COMMUNICATION

Cite this: *Phys. Chem. Chem. Phys.*, 2015, **17**, 3000

Received 23rd September 2014,
Accepted 8th December 2014

DOI: 10.1039/c4cp04279d

www.rsc.org/pccp

Fullerene-like boron clusters stabilized by an endohedrally doped iron atom: B_nFe with n = 14, 16, 18 and 20†

Nguyen Minh Tam,[ab] Hung Tan Pham,[a] Long Van Duong,[a] My Phuong Pham-Ho[a] and Minh Tho Nguyen*[b]

Stabilized fullerene and tubular forms can be produced in boron clusters B_n in small sizes from $n \sim 14$ to 20 upon doping by transition metal atoms. $B_{14}Fe$ and $B_{16}Fe$ are stable tubes whereas $B_{18}Fe$ and $B_{20}Fe$ are stable fullerenes. Their formation and stability suggest the use of dopants to induce different growth paths leading to larger cages, fullerenes and tubes of boron.

Boron compounds exhibit extremely rich structural features. In the solid state, elemental boron is well-known to exist in the form of amorphous, α- and β-rhombohedral allotropes, and in boron-rich compounds such as boranes and their numerous derivatives. Aggregates of the boron elements such as clusters,[1] sheets[2] and nanotubes[3–5] have been prepared or predicted, and indeed they showed many structural peculiarities.[6]

Concerning gas phase boron clusters B_n, a plethora of two-dimensional (2D, planar and quasi-planar) and three-dimensional (3D, tubular, cage, spherical, fullerene…) shapes were identified, suggesting several distinct growth patterns.[7–15] In relation to C_{60}, particular attention has been paid to the boron buckyball B_{80},[16–19] and the larger fullerene derivatives such as B_{100}[2,20] and B_{112}.[21] A number of smaller all-boron fullerenes were also identified by computations including B_{14}, B_{32}, B_{38}, B_{40}, B_{44}, B_{50} and B_{56}.[12,22–29] The B_{30} cluster was demonstrated to have a bowl-shaped ground state structure, and the bowl B_{30} constitutes an appropriate building-block whose recombination and addition could eventually lead to the generation of B_{80}, B_{90} and B_{92} buckyballs.[29] Of the smaller boron clusters, the B_{14} and B_{40} fullerene-like neutral species were found to be the global minima at these sizes.[12,24]

A B_{40} fullerene-type is characterized by two hexagonal faces and in particular four heptagonal faces. It has a high symmetry (D_{2d}) in which the C_2 axis is going through the two hexagons. The MOs of this fullerene-like B_{40} closely mimic those of the buckyball B_{80}.[24] Such a B_{40} fullerene was recently observed by experiment using photoelectron spectroscopy.[26]

Interest in small finite-size and stable fullerenes led to intensive search for novel building blocks for nanostructures. In this respect, the doping of a cluster has often been used to stabilize and modify the structure and properties of the resulting doped cluster. For some specific sizes, the dopant can drastically alter not only the thermochemical stability, but also electronic and magnetic properties.[30–33] Doping by metallic elements was frequently used to compensate the inherent electron deficiency of boron atoms. In the typical case of MgB_2, the Mg dopant injects electrons into the hexagonal B network in such a way that the electron transfer makes the Mg-doped boron semiconductors behave like a carbon graphite.[6]

Along these lines, a number of small planar cyclic boron clusters doped by transition metals have been reported. These include the B_8M^-, B_9M^- with M = Co, Fe, Ni,[34,35] or 3rd period elements.[36] In the series of B_nM^- with n = 3–10 and M = V and Ta, these doped anionic clusters were observed experimentally, but the doped clusters also exhibit different shapes ranging from 3D (boat-like, pyramid-like) to 2D molecular wheels in which the boron atom is basically multi-coordinated. There is a competition between B–B and M–B interaction in determining the most stable structures of the doped clusters. It is clear that with such small sizes, no cage-like or fullerene-like boron structures could be formed. Endohedral doping of the buckyball B_{80} by transition metals, or organic species[37] has also been explored, but in such a large hollow medium, chemical reactions could often occur.

Recently, we found that small size clusters such as Si_8,[38] Si_{10},[39] Ge_{12}[40] and Si_{14}[41] can already encapsulate a metallic element such as Be, Co, Li and Mn giving quite stabilized doped clusters Si_8Be, $Si_{10}Co$, $Ge_{12}Li^+$ and $Si_{14}Mn^+$, respectively, in such a way that the resulting endohedrally doped clusters correspond to the lowest-lying isomers, and the high spin of the metallic dopant could completely be quenched. In this context, we set out to search for small size fullerene-like boron clusters that could be stabilized

[a] *Institute for Computational Science and Technology (ICST), Ho Chi Minh City, Vietnam*
[b] *Department of Chemistry, University of Leuven, Leuven, Belgium. E-mail: minh.nguyen@chem.kuleuven.be*

† Electronic supplementary information (ESI) available: Computational methods. Figures contain shape and relative energies of the lower-lying isomers. The orbital interaction diagrams, the total and partial DOS maps. See DOI: 10.1039/c4cp04279d

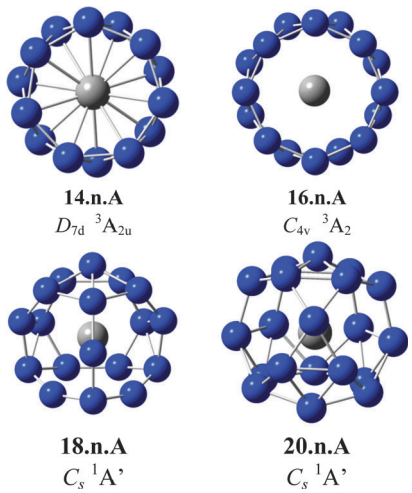

Fig. 1 Shapes, point group and electronic states of the most stable isomers B_nFe with n = 14, 16, 18, 20 obtained using TPSSh/6-311+G(d) computations.

following endohedral doping by transition metals by using a similar strategy.

Considering the fact that B_{14} has already a stable fullerene-like geometry, and B_{20} has a double ring tube, we thus take the series of B_{14}, B_{16}, B_{18} and B_{20}, and then dope them successively with different first-row transition metals ranging from Sc to Cu. For each metallic element, we considered different charge and spin states. In the present communication, we report the promising results obtained for the iron doped boron clusters B_nFe, which reveal some novel structural and electronic features. We first search for lower-lying structures, and subsequently analyze their bonding phenomena.

Computational methods are given in the ESI.† We used density functional theory with the TPSSh and B3P86 functionals in conjunction with the 6-311+G(d) basis set for geometries, frequencies and energies. Geometries and relative energies of the lower-lying isomers are given in the ESI.† The shapes of the lowest lying isomers of $B_{14}Fe$, $B_{16}Fe$, $B_{18}Fe$ and $B_{20}Fe$ are displayed in Fig. 1. The results obtained by both functionals are similar to each other. To simplify the presentation of data, only TPSSh results are given hereafter. Let us first briefly describe the structural and energetic aspects of the doped B_nFe clusters.

(i) $B_{14}Fe$ clusters

The energy ordering of the four lowest-lying isomers is displayed in the Fig. S1 of the ESI.† Each of the two most stable isomers corresponds to a double ring (DR) composed of two seven-membered rings in an anti-prism form and doped by the Fe atom at the center of the cylinder. The high symmetry (D_{7d}) and high spin $^3A_{2u}$ **14-n-A** (Fig. 1) turns out to be ~0.1 eV more stable than the low-spin counterpart. Interaction of the Fe atom with the fullerene-like B_{14} structure does not lead to a low-energy fullerene adduct but the resulting doped cluster has a semi-closed low spin structure (**B14.Fe.n.C**, C_{2v}, $^1A_1$, Fig. S1, ESI†). The overall effect of Fe attachment to B_{14} is the emergence of the DR as the lowest-lying structure.

(ii) $B_{16}Fe$ clusters

The energy ordering of $B_{16}Fe$ clusters calculated using the TPSSh functional is shown in Fig. S2 of the ESI,† in which **16.n.A** (C_{4v}, $^3A_2$) structure is the most stable isomer. The pure B_{16} cluster exhibits a symmetrical planar shape (C_{2h}, ^1A_g)[8] which is ~7 kcal mol^{-1} higher in energy (PBE/6-311+G(d)+ZPE) than the DR form composed of two eight-membered rings. As in the previous case, attachment of a Fe atom favours the doped-DR form. The triplet state **16-n-A** shown in Fig. 1 is preferred over a distorted low-symmetry closed-shell state and a high symmetrical quintet state (Fig. S2 of the ESI†).

Fig. 2 displays the partial and total densities of states (DOS) of the triplet DR **16-n-A** in which the α and β spin molecular orbitals are separately plotted. This illustrates a clear picture of its electronic shell. As expected, the frontier MOs are composed mainly of the 2p(B) and 3d(Fe) AOs, but with a larger component of the boron AOs. Its HOMO and LUMO however arise exclusively from the boron AOs. An orbital interaction correlation diagram (displayed in Fig. S5 of the ESI†) clearly points out the stabilization of the adduct due to orbital interactions.

(iii) $B_{18}Fe$ clusters

Two singlet planar structures were found to have similar energy content and thus compete for the ground state of the pure B_{18}.[8] They are a few kcal mol^{-1} lower in energy than a distorted DR formed by a superposition of two nine-membered rings. The DR turns out to be the lowest-energy structure of the cation B_{18}^+.[8] The relative energy ordering of the four lower-lying $B_{18}Fe$ isomers (Fig. S3, ESI†) is rather method-dependent, but the endohedrally doped cage **18-n-A** (C_s, Fig. 1) remains favoured over the other isomers. The Fe dopant tends to stabilize the cage and DR forms of B_{18} more than the planar counterparts, in

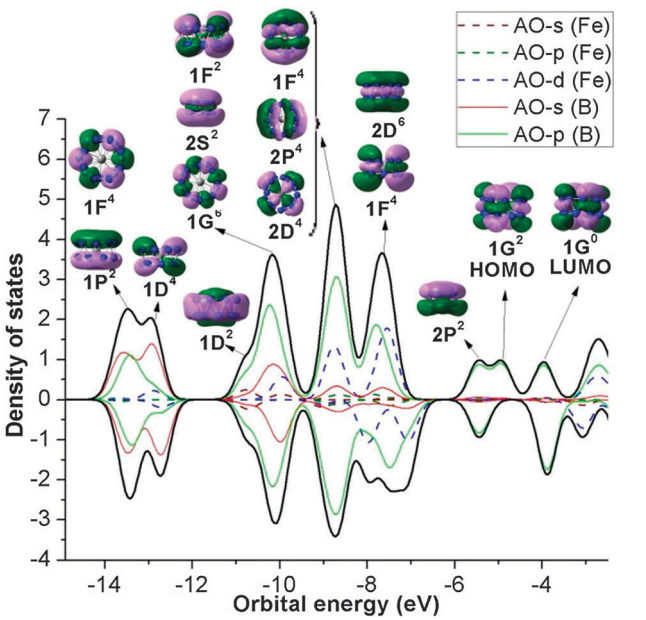

Fig. 2 Total (DOS) and partial (pDOS) densities of state of $B_{16}Fe$ **16-n-A**. The shapes of MOs are obtained using TPSSh/6-311+G(d) computations.

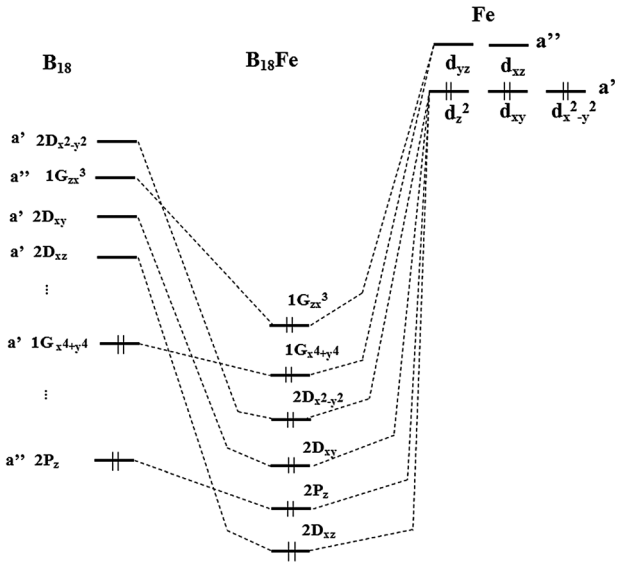

Fig. 3 Orbital interaction diagram between a fullerene-like B_{18} cage and the Fe atom giving the doped cluster $B_{18}Fe$ **18.n.A**.

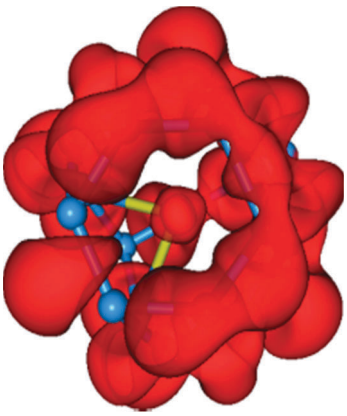

$B_{18}Fe$ 18-n-A

Fig. 4 The ELF iso-surface at a bifurcation value of 0.85 of the doped $B_{18}Fe$ cluster. The wave functions were obtained using the TPSSh/6-311+G(d) computations.

making the endohedrally doped **18-n-A** a lower-lying isomer. The emergence of the low-spin fullerene-like form **18-n-A** thus constitutes a remarkable effect of Fe doping. In return, the high spin of the Fe atom is thus completely quenched following its endohedral doping. The orbital correlation diagram displayed in Fig. 3 again indicates the strong stabilization of the resulting $B_{18}Fe$ MOs.

(iv) $B_{20}Fe$ clusters

It is well established that the lowest-lying isomer of the bare B_{20} is characterized by a DR shape,[8,9] even though the energy difference between both corresponding DR and planar counterparts is relatively small, being $\sim$5–8 kcal mol^{-1} depending on the method employed. The doped DR **20-n-B** (Fig. S4 of the ESI†) has a distorted shape with an asymmetrical position of the dopant within the cylinder. This is presumably due to the fact that the space inside the B_{20} DR is too large, and thereby the B–Fe distances too long, to accommodate a symmetrical Fe atom at the center. Overall, similar to the $B_{18}Fe$ **18-n-A** structure, the emergence of an endohedrally doped fullerene-type **20-n-A** (Fig. 1) having a closed-shell electronic state represents an important effect of the Fe doping. The total (DOS) and partial (pDOS) densities of states illustrated in Fig. S6 (ESI†) clearly point out the overlap between d orbitals of Fe and both s and p orbitals of B atoms.

The electron localization function (ELF) plot of $B_{18}Fe$ displayed in Fig. 4 shows a high ELF value of 0.85 indicating strong interaction between skeletal B_{18} bonds and the Fe dopant. No localization domains can be found between the Fe atom and B_{18} counterparts, suggesting a certain ionic character of the Fe–B bonds. The NBO charge of the Fe atom in $B_{18}Fe$ is about -1.0 electron in the singlet fullerene. Thus the B_{18} cage actually transfers electrons to the Fe atom, and the $B_{18}Fe$ cage can be seen to involve anion Fe^- and cation B_{18}^+ fullerene. Electrostatic interaction also contributes to its thermodynamic stability. Such a situation is not uncommon. In the Mn-doped silicon fullerene $Si_{14}Mn^+$, a charge transfer is also found to take place from the Si_{14} moiety to the dopant.[41]

In summary, the most interesting result of our extensive search for the M-doped B_nM clusters is the finding that strong effects of the Fe dopant substantially stabilize the double ring shape from the size of 14 (**14-n-A**) and 16 (**16-n-A**), and the fullerene-like shape from the size of 18 (**18-n-A**) and 20 (**20-n-A**). Overall, stabilized fullerene and tubular adducts can be formed in boron clusters B_n in the smaller size range, in which the high spin of the dopant atom is partially quenched already from the sizes of 14 and 16, and completely quenched at the sizes of 18 and 20. Their formation foreshadows different growth paths leading to larger boron cages, tubes and fullerenes.

Notes and references

1 L. Hanley and S. L. Anderson, *J. Phys. Chem.*, 1987, **91**, 5161.
2 C. Ozdogan, S. Mukhopadhyay, W. Hayami, Z. B. Guvenc, R. Pandey and I. Boustani, *J. Phys. Chem. C*, 2010, **114**, 4362.
3 G. Ciofani, V. Raffa, A. Menciassi and A. Cuschieri, *Nano Today*, 2009, **4**, 8.
4 A. K. Singh, A. Sadrzdeh and B. I. Yakobson, *Nano Lett.*, 2008, **8**, 1314.
5 I. Boustani, A. Quandt, E. Hernandez and A. Rubio, *J. Chem. Phys.*, 1999, **110**, 3176.
6 H. Tang and S. Ismail-Beigi, *Phys. Rev. Lett.*, 2007, **99**, 115501.
7 S. Chacko, D. G. Kanhere and I. Boustani, *Phys. Rev. B: Condens. Matter Mater. Phys.*, 2003, **68**, 035414.
8 T. B. Tai, M. N. Tam and M. T. Nguyen, *Chem. Phys. Lett.*, 2012, **530**, 71.
9 B. Kiran, S. Bulusu, H. J. Zhai, S. Yoo, X. C. Zeng and L. S. Wang, *Proc. Natl. Acad. Sci. U. S. A.*, 2005, **102**, 961.
10 H. T. Pham, L. V. Duong, B. Q. Pham and M. T. Nguyen, *Chem. Phys. Lett.*, 2013, **577**, 32.
11 L. Jian, Y. Wang, L. Zhu and Y. Ma, *Nanoscale*, 2014, **6**, 11692.

12 L. Cheng, *J. Chem. Phys.*, 2012, **136**, 104301.
13 E. Oger, N. R. M. Crawford, R. Kelting, P. Weis, M. M. Kappes and R. Ahlrichs, *Angew. Chem., Int. Ed.*, 2007, **46**, 8503.
14 T. B. Tai, N. M. Tam and M. T. Nguyen, *Theor. Chem. Acc.*, 2012, **131**, 1241.
15 N. G. Szwacki, A. Sadrzadeh and B. I. Yakobson, *Phys. Rev. Lett.*, 2007, **98**, 166804.
16 J. T. Muya, E. Lijnen, M. T. Nguyen and A. Ceulemans, *J. Phys. Chem. A*, 2011, **155**, 2268.
17 J. T. Muya, H. Ramanantoanina, C. Daul, M. T. Nguyen, G. Gopakumar and A. Ceulemans, *Phys. Chem. Chem. Phys.*, 2013, **15**, 2829.
18 D. E. Bean, J. T. Muya, P. W. Fowler, M. T. Nguyen and A. Ceulemans, *Phys. Chem. Chem. Phys.*, 2011, **13**, 20855.
19 H. He, R. Pandey, I. Boustani and S. P. Karna, *J. Phys. Chem. C*, 2010, **114**, 4149.
20 J. T. Muya, G. Gopakumar, M. T. Nguyen and A. Ceulemans, *Phys. Chem. Chem. Phys.*, 2011, **13**, 7524.
21 L. Wang, J. Zhao, F. Li and Z. Chen, *Chem. Phys. Lett.*, 2010, **501**, 16.
22 H. Lu and S. Li, *J. Chem. Phys.*, 2013, **139**, 224307.
23 S. Botti, A. Castro, N. N. Lathiotakis, X. Andrade and M. A. L. Marques, *Phys. Chem. Chem. Phys.*, 2009, **11**, 4523.
24 H. T. Pham, L. V. Duong, N. M. Tam, M. P. Pham-Ho and M. T. Nguyen, *Chem. Phys. Lett.*, 2014, **608**, 295.
25 X. Sheng, Q. Yan, Q. Zheng and G. Su, *Phys. Chem. Chem. Phys.*, 2009, **11**, 9696.
26 H. J. Zhai, Y. F. Zhao, W. L. Li, Q. Chen, H. Bai, H. S. Hu, Z. A. Piazza, W. J. Tian, H. G. Lu, Y. B. Wu, Y. W. Mu, G. F. Wei, Z. P. Liu, J. Li, S. D. Li and L. S. Wang, *Nat. Chem.*, 2014, **6**, 727.
27 K. D. Quarles, C. B. Kah, R. N. Gunasinghe, R. N. Musin and X. Wang, *J. Chem. Theory Comput.*, 2011, **7**, 2017.
28 W. Hayami and S. Otani, *J. Phys. Chem. A*, 2011, **115**, 8204.
29 T. B. Tai, L. V. Duong, H. T. Pham, D. T. T. Mai and M. T. Nguyen, *Chem. Commun.*, 2014, **50**, 1558.
30 S. De, A. Willand, M. Amsler, P. Pochet, L. Genovese and S. Goedecker, *Phys. Rev. Lett.*, 2011, **106**, 225502.
31 P. Boulanger, M. Morinere, L. Genovese and P. Pochet, *J. Chem. Phys.*, 2013, **138**, 184302.
32 E. Janssens, H. Tanaka, S. Neukermans, R. E. Silverans and P. Lievens, *Phys. Rev. Lett.*, 2004, **90**, 033401.
33 C. Buzea and T. Yamashiat, *Supercond. Sci. Technol.*, 2001, **14**, R115.
34 K. Ito, Z. Pu, Q. Li and P. v. R. Scheyer, *Inorg. Chem.*, 2008, **47**, 10906.
35 Y. Liao, C. L. Cruz, P. v. R. Schleyer and Z. Chen, *Phys. Chem. Chem. Phys.*, 2012, **14**, 14898.
36 W. Li, A. S. Ivanov, J. Federic, C. Romanescu, I. Cernusak, A. I. Boldyrev and L. S. Wang, *J. Chem. Phys.*, 2013, **139**, 104312.
37 J. T. Muya, E. Lijnen, M. T. Nguyen and A. Ceulemans, *J. Phys. Chem. A*, 2011, **115**, 2268.
38 V. T. Ngan and M. T. Nguyen, *J. Phys. Chem. A*, 2010, **114**, 7609.
39 Y. Li, N. M. Tam, P. Claes, A. P. Woodham, J. T. Lyon, V. T. Ngan, M. T. Nguyen, P. Lievens, A. Fielicke and E. Janssens, *J. Phys. Chem. A*, 2014, **118**, 8198.
40 T. B. Tai and M. T. Nguyen, *Chem. Phys. Lett.*, 2010, **492**, 290.
41 V. T. Ngan, K. Pierloot and M. T. Nguyen, *Phys. Chem. Chem. Phys.*, 2013, **15**, 5493.